

1 **The double dip: how tropospheric expansion**
2 **counteracts increases in extratropical stratospheric**
3 **ozone under global warming**

4 **Aaron Match¹, Edwin P. Gerber¹**

5 ¹Center for Atmosphere Ocean Science, Courant Institute of Mathematical Sciences, New York University

6 **Key Points:**

- 7 • Under increasing CO₂, models project extratropical stratospheric ozone to increase
8 except around 10 km (lower dip) and 17 km (upper dip).
- 9 • The lower dip is due to expansion of the extratropical troposphere, whereas the
10 upper dip is due to expansion of the tropical troposphere.
- 11 • The lower dip is strongest in winter when ozone is greatest. The upper dip is strongest
12 in summer when Brewer-Dobson downwelling is weakest.

Corresponding author: Aaron Match, aaron.match@nyu.edu

Abstract

In response to rising CO₂, chemistry-climate models project that extratropical stratospheric ozone will increase, except around 10 km and 17 km. We call the muted increases or reductions at these altitudes the “double dip”. The double dip results not from stratospheric cooling but from surface warming. Using an idealized photochemical-transport model, surface warming is found to produce the double dip via tropospheric expansion, which converts ozone-rich stratospheric air into ozone-poor tropospheric air. The lower dip results from expansion of the extratropical troposphere, as previously understood. The upper dip results from expansion of the *tropical* troposphere, low-ozone anomalies from which are then transported into the extratropics. Large seasonality in the double dip in chemistry-climate models can be explained by seasonality in the Brewer-Dobson circulation. The remote effects of the tropical tropopause on extratropical ozone complicate the use of (local) tropopause-following coordinates to remove the effects of global warming.

Plain Language Summary

In response to rising atmospheric CO₂ primarily from the burning of fossil fuels, beneficial ozone in the mid-latitude stratosphere tends to increase due to changes in the winds and temperature-dependent reaction rates. However, these broad increases in ozone are punctuated by reductions (or muted increases) around 10 km and 17 km, which we term the “double dip”. We find that the double dip exists because the warming of the troposphere allows the tops of rainclouds to reach higher altitudes, reducing stratospheric ozone through the injection of ozone-poor tropospheric air. The lower dip around 10 km results intuitively from the deepening of the mid-latitude troposphere. Counterintuitively, the upper dip around 17 km results from deepening of the faraway tropical troposphere, whose remote reductions in tropical ozone are then transported laterally over the mid-latitudes. Thus, the double dip depends on both the local and remote deepening of the troposphere, which could complicate a common practice of filtering out the effects of tropospheric expansion that only considers the local component.

1 Introduction

Whereas the largest anthropogenic effects on the ozone layer have resulted from chemical perturbations due to ozone-depleting substances, the ozone layer is also being

44 perturbed thermodynamically and dynamically due to rising CO₂. Rising CO₂ leads to
45 both increases and decreases in ozone at different locations, and chemistry-climate mod-
46 els (CCMs) robustly agree on the spatial pattern of this response (e.g., Haigh & Pyle,
47 1982; Shepherd, 2008; Chiodo et al., 2018; Match & Gerber, 2022). Examples of this ro-
48 bust response are shown from three CCMs in Fig. 1. Ozone is simulated to increase in
49 the mid- to upper-stratosphere (i.e., above the ozone maximum), because stratospheric
50 cooling speeds up the three-body reaction that forms O₃ and slows down certain colli-
51 sional loss reactions (Haigh & Pyle, 1982; Jonsson et al., 2004). Ozone is simulated to
52 decrease in the tropical lower stratosphere for two main reasons: (1) a strengthening of
53 the Brewer-Dobson circulation (BDC), which upwells ozone-poor air from below (e.g.,
54 Shepherd, 2008; Li et al., 2009), and (2) tropospheric expansion, which erodes the ozone
55 layer from below to lead to reductions of ozone that are then upwelled by the climato-
56 logical BDC (Match & Gerber, 2022).

57 The ozone response in the extratropical lower stratosphere is less straightforward,
58 as it is not uniform in sign, and, unlike the changes elsewhere, exhibits some sign asym-
59 metries between hemispheres and sign disagreements between models (Fig. 1). Nonethe-
60 less, a robust vertical structure of the response is evident: although ozone generally in-
61 creases in the extratropical lower stratosphere under global warming, these increases are
62 punctuated by two “dips” (i.e., reductions in the magnitude of the increase possibly ris-
63 ing to the level of an absolute decrease): a *lower dip* around 10 km and an *upper dip* around
64 17 km. We call this response the “double dip”. The double dip exists when averaging
65 either poleward of 30°, where the upper dip might be contaminated by a direct contri-
66 bution from ozone reductions in the tropical upwelling regime, or when averaging pole-
67 ward of 60°, far from any tropical contamination (Fig. 1, bottom row, solid vs. dashed
68 curves).

69 The lower dip has been previously described and attributed to tropospheric expan-
70 sion, which erodes the ozone layer from below by replacing ozone-rich stratospheric air
71 with ozone-poor tropospheric air (Plummer et al., 2010; Dietmüller et al., 2014). The
72 upper dip, on the other hand, has not been the focus of prior work and has not been ex-
73 plicitly discussed despite appearing (sometimes subtly) in figures from numerous pre-
74 vious studies, including Fomichev et al. (2007, their Fig. 12), Shepherd (2008, their Fig.
75 11), Plummer et al. (2010, their Fig. 2), Dietmüller et al. (2014, their Fig. 1a), Banerjee
76 et al. (2016, their Fig. 1), Chiodo et al. (2018, their Fig. 2), and Keeble et al. (2021, their

77 Fig. 10). Our goals are to explain the mechanisms that lead to the double dip and frame
78 their implications for interpreting ozone trends in the extratropical lower stratosphere.

79 We begin by analyzing pairs of CMIP6 experiments that isolate the two pathways
80 by which rising CO₂ affects ozone: stratospheric cooling and surface warming. The dou-
81 ble dip will be found to result from surface warming (Section 2). Surface warming is *a*
82 *priori* understood to affect stratospheric ozone through tropospheric expansion and by
83 strengthening the BDC (the latter arguably connected to the former, e.g., as in Oberländer-
84 Hayn et al. (2016), although our analysis treats their effects separately). To disentangle
85 the effects of tropospheric expansion and the strengthening BDC, we analyze a highly
86 simplified photochemical-transport model within which the tropopause height and BDC
87 strength can be independently varied, an extension of that developed by Match and Ger-
88 ber (2022) (Section 3). Our results support previous arguments that the lower dip arises
89 from expansion of the extratropical troposphere (Plummer et al., 2010; Dietmüller et al.,
90 2014) (Section 4). The upper dip also arises from tropospheric expansion, but not of the
91 (local) extratropical troposphere but rather of the *tropical* troposphere, reductions in ozone
92 from which are then laterally transported into the extratropics at the altitude of the trop-
93 ical tropopause around 17 km. We proceed to explain seasonality in the double dip as
94 a consequence of the seasonal cycle of the BDC (Section 5), then discuss implications
95 of these results for the interpretation of tropopause-following coordinates (Section 6).

96 **2 The double dip: surface warming, not stratospheric cooling**

97 The extratropical ozone response to a quadrupling of CO₂ is shown in Fig. 1, and
98 for a quantitative comparison among CCMs in Fig. 2a. The increase of CO₂ is thought
99 to affect the ozone layer by perturbing the thermodynamical and dynamical conditions
100 that determine ozone reaction rates and transport. These effects can be distinguished
101 by considering the separate effects of stratospheric cooling and surface warming, whose
102 contributions to the double dip can be assessed by comparing pairs of chemistry-climate
103 model experiments that isolate each in turn (similar decompositions appear in, e.g., Fomichev
104 et al., 2007; Match & Gerber, 2022). These pairs of experiments are drawn by oppor-
105 tunity from the CMIP6 archive. The pairs of experiments have slightly different back-
106 ground states, pre-industrial for isolating stratospheric cooling versus historical for iso-
107 lating surface warming.

108 Surface warming is isolated by comparing two experiments with prescribed sea sur-
109 face temperatures (SSTs). A standard experiment with prescribed historically-evolving
110 SSTs (amip) is compared to one in which those historical SSTs are uniformly warmed
111 by 4 K (amip-p4K). Warming the SSTs warms the troposphere, but does not lead to strato-
112 spheric cooling, which occurs under rising CO₂ due to the direct radiative effects of the
113 enhanced CO₂ in the stratosphere (Manabe & Wetherald, 1967). Surface warming ex-
114 pands the troposphere and strengthens the BDC. Fig. 2b shows the extratropical ozone
115 response to surface warming in three CCMs. Surface warming also leads to a pronounced
116 double dip, with localized reductions around 10 km and 17 km.

117 To determine whether stratospheric cooling also contributes to the double dip, we
118 isolate its effects. Stratospheric cooling is isolated by comparing a control experiment
119 (piControl) to an experiment in which CO₂ is quadrupled while holding SSTs fixed (piClim-
120 4xCO₂). The increase of CO₂ increases the radiative cooling of the stratosphere to lead
121 to stratospheric cooling, whereas the warming effects of the CO₂ in the troposphere are
122 suppressed by keeping surface temperatures fixed. Fig. 2c shows that stratospheric cool-
123 ing leads to an increase in extratropical ozone above about 17 km, primarily by perturb-
124 ing the photochemical reaction rates that produce and destroy ozone. The ozone response
125 in the extratropical lower stratosphere is small, and there is no evidence of reductions
126 that would project significantly onto either the upper or lower dip. Therefore, we con-
127 clude that the double dip results primarily from surface warming.

128 **3 Methods: A simple model to disentangle contributions from the Brewer-** 129 **Dobson circulation and tropospheric expansion**

130 In order to understand how surface warming leads to the double dip, it is neces-
131 sary to mechanistically disentangle its two primary pathways for affecting ozone: tro-
132 pospheric expansion and strengthening of the Brewer-Dobson circulation. Tropospheric
133 expansion is a direct thermodynamic consequence of global warming (Singh & O’Gorman,
134 2012; Vallis et al., 2015). Based on the idea that convection must deepen in order for a
135 moist adiabatic parcel launched at the surface to reach an approximately fixed tropopause
136 temperature (Hartmann & Larson, 2002; Seeley et al., 2019; Jeevanjee & Fueglistaler,
137 2020; McKim et al., 2024), Match and Fueglistaler (2021) derived a simple scaling for
138 tropospheric expansion of 6 hPa per Kelvin of surface warming. The strengthening Brewer-
139 Dobson circulation is a circulation response that also scales with surface warming, and

140 Oberländer-Hayn et al. (2016) have argued that it is a direct consequence of the upward
141 shift of the circulation under tropospheric expansion, although we can assess their ef-
142 fects independently. To do so, we formulate an idealized photochemical-transport model
143 that distills the processes that control extratropical stratospheric ozone, but allows us
144 to independently prescribe values for the tropopause height and BDC strength.

145 The model is a Chapman+2 photochemical-transport model, and its formulation
146 draws from two streams of previous work. From the first stream, we adopt a Chapman
147 Cycle-based model of spectrally-resolved UV photochemistry in an isothermal atmosphere
148 with transport between the tropics and extratropics via a leaky tropical pipe, and zero
149 ozone below the prescribed tropopause (Match & Gerber, 2022). From the second stream,
150 we augment our Chapman Cycle reactions with two additional reactions representing gen-
151 eralized catalytic sinks of O and O₃ (the Chapman+2 model: Match et al., 2024a, 2024b).
152 The rates of these generalized catalytic sinks depend on the climatological distribution
153 of catalysts drawn from a chemistry-climate model as tabulated in Brasseur and Solomon
154 (2005). The Chapman+2 model has previously been described in a steady-state formu-
155 lation with transport parameterized as a damping in the above reference, but here we
156 represent transport explicitly using the leaky tropical pipe. To produce a realistic an-
157 nual cycle of the double dip, we split the extratropics into a Northern Hemisphere col-
158 umn and a Southern Hemisphere column, and impose an annual cycle in the strength
159 of the BDC, which peaks in the winter in each hemisphere.

160 The leaky tropical pipe is generally formulated to represent the mid- to upper-stratosphere,
161 where the tropics are isolated from the extratropics (Neu & Plumb, 1999). In order to
162 extend the leaky tropical pipe down to lower altitudes, we impose a jump towards larger
163 lateral mixing below the tropical tropopause, which has the effect of damping ozone in
164 the extratropical lower stratosphere and could be interpreted to represent known lateral
165 mixing pathways above the subtropical jet (e.g. Hoor et al., 2004; Gettelman et al., 2011).

166 A schematic showing the basic formulation of the resulting Chapman+2 photochemical-
167 transport model is shown in Fig. S1. A detailed description of the model and our nu-
168 merical approach is provided in Texts S1 and S2. The climatological seasonal cycle of
169 ozone in our model is shown in Fig. S2, indicating a favorable comparison to that from
170 the chemistry-climate model MRI-ESM2-0.

171 Perturbations are applied to the Chapman+2 photochemical transport model to
172 represent the three key effects of rising CO₂. Stratospheric cooling, represented as a uni-
173 form cooling of 10 K, perturbs the temperature-dependent reaction rates for the Chap-
174 man+2 reactions. Strengthening of the Brewer-Dobson circulation, represented by a uni-
175 form increase of \bar{w}^* by 0.05 mm s⁻¹, perturbs transport by the leaky tropical pipe. Tro-
176 pospheric expansion, represented by a 1 km upward shift of the tropopause and lateral
177 mixing, takes a bite out of the ozone layer from below that is then transported by ad-
178 vection and mixing. Together, these perturbations will be shown to approximate the re-
179 sponse to a quadrupling of CO₂ (see also Match & Gerber, 2022). Critically for our un-
180 derstanding, they can be imposed separately or in various combinations to emulate ex-
181 periments from the CMIP6 models, allowing us to assess the linearity of the response,
182 and ultimately disentangle the relative contributions to the double dip.

183 Omitted in our model is another proposed decadal driver of extratropical ozone trends:
184 changes in the latitudinal structure of two-way mixing. An idealized model suitable to
185 represent such changes would require higher latitudinal resolution. This caveat prevents
186 our model from reproducing this particular proposed mechanism for recent unexpected
187 declines in extratropical lower stratospheric ozone (Ball et al., 2018; Wargan et al., 2018;
188 Ball et al., 2020; Orbe et al., 2020).

189 **4 Results: The double dip is due to tropospheric expansion**

190 The Chapman+2 photochemical-transport model was designed to emulate the ex-
191 tratropical ozone changes in chemistry-climate models in response to surface warming
192 and/or stratospheric cooling. To establish its fitness, we show three validation bench-
193 marks, one in each row of Fig. 2. The model successfully reproduces the qualitative struc-
194 ture of the extratropical stratospheric ozone response to each perturbation. In response
195 to simultaneous surface warming and stratospheric cooling, ozone increases aloft and there
196 is a double dip in the lower stratosphere (Fig. 2a vs. 2d). Isolating the response to sur-
197 face warming retains the double dip, now with only small ozone changes above 20 km
198 (Fig. 2b vs. 2e). Isolating the response to stratospheric cooling retains the increased ozone
199 above 20 km, but without the double dip (Fig. 2c vs. 2f).

200 The success of the Chapman+2 model in these mechanism denial experiments builds
201 confidence that it can also further decompose the response to surface warming into the

202 distinct effects of a strengthening BDC and tropospheric expansion. This decomposition
203 is shown in Figs. 2d and 2e. Consistent with prior literature, the strengthening BDC (ma-
204 genta curves) increases ozone in the extratropical lower stratosphere (e.g., Shepherd, 2008).
205 These increases arise from stronger downwelling of ozone-rich air that can equilibrate
206 at a higher concentration against sinks from photochemistry and mixing. The leaky trop-
207 ical pipe framework also captures the increase in lateral transport from tropics to ex-
208 tratropics. Potential reductions of extratropical ozone from this enhanced lateral trans-
209 port of ozone-poor air from the tropics are overwhelmed by the increases of ozone from
210 enhanced downwelling.

211 With the strengthening BDC leading to broad increases of ozone, the double dip
212 must instead result from tropospheric expansion (Fig. 2d and 2e, red and cyan curves).
213 As others have argued, expansion of the extratropical troposphere leads directly to the
214 lower dip by eroding the ozone layer from below (Plummer et al., 2010; Dietmüller et
215 al., 2014) (cyan curves). A new result of this figure is that the upper dip comes from ex-
216 pansion of the *tropical* troposphere (red curves). The expanding tropical tropopause erodes
217 the ozone layer in the tropical lower stratosphere, low ozone anomalies from which are
218 then advected and mixed into the extratropical lower stratosphere. As represented in our
219 model, tropical tropospheric expansion induces an upper dip due to both the upward shift
220 in tropical tropospheric destruction of ozone and the upward shift in the lateral mixing
221 profile that jumps to larger values below the tropical tropopause. These two effects both
222 contribute at leading order, as seen in the decomposition of Fig. S3. In total, the column-
223 integrated response to (remote) tropical tropospheric expansion is not only significant
224 but is actually several factors larger than the response to (local) extratropical tropospheric
225 expansion.

226 The double dip is thus a function of both local (extratropical) and remote (trop-
227 ical) tropospheric expansion. The lower dip occurs around 10 km at the altitude of the
228 extratropical tropopause, and the upper dip is centered around 17 km at the altitude of
229 the tropical tropopause. The gap of approximately 7 km separating the two dips there-
230 fore reflects the tropopause break in the vicinity of the subtropical jet, whereby the tropopause
231 drops discontinuously between the tropics and the extratropics. A pathway of lateral mix-
232 ing from the tropical lower stratosphere into the extratropical lower stratosphere has pre-
233 viously arisen in other contexts, such as when considering transport of short-lived sub-

stances and idealized tracers (Hoor et al., 2004; Bönisch et al., 2009; Gettelman et al., 2011; Abalos et al., 2017).

These results suggest that tropospheric expansion is uniquely responsible for the double dip. This result is quantitative but also qualitative; the strengthening BDC and stratospheric cooling strictly increase ozone without imparting much structure from the tropopause onto their responses, whereas tropospheric expansion strictly reduces ozone while strongly imprinting tropopause structure. The singular role of tropospheric expansion in leading to the double dip can be contrasted to the case of tropical ozone changes under global warming, in which tropospheric expansion and the strengthening BDC reinforce each other in leading to reductions of ozone (Match & Gerber, 2022), making the attribution of their relative contributions a quantitative question.

5 Results: Seasonality of the double dip due to seasonality of the Brewer-Dobson circulation

So far, we have presented results and mechanistic arguments that appeal to the annually-averaged double dip. However, the double dip is not predicted in CCMs to exist year-round. Figs. 3a (Northern Hemisphere) and S4a (Southern Hemisphere) show that the lower dip is strongest in winter, whereas the upper dip is strongest in summer and vanishes in winter. This seasonal cycle is evident in both hemispheres and in other chemistry-climate models (Fig. S5). Compared to the time-averaged double dip, the seasonal cycle provides a more stringent test of our explanatory framework.

There are many seasonally-varying aspects of ozone photochemistry and transport that could be important for the modulating the double dip. On the photochemistry side, there are annual cycles in solar zenith angle, catalyst concentrations, and temperature-dependent reaction rates, among others. On the transport side, there are annual cycles in tropopause height and the strength of the Brewer-Dobson circulation, which is strongest in winter due to the enhanced planetary wave activity propagating up from the troposphere (e.g., Holton et al., 1995; Butchart, 2014). There is also an annual cycle in the lateral mixing from the tropical tropopause layer above the subtropical jet into the extratropical lower stratosphere, which maximizes during summer associated with the Asian summer monsoon anticyclone (e.g. Hoor et al., 2004; Gettelman et al., 2011; Stolarski et al., 2014). Although all of these photochemical and transport factors could in principle contribute significantly to the seasonal cycle in the double dip, here we show that

266 just one factor—the seasonal cycle in BDC strength—is sufficient to reproduce the sea-
267 sonality of the double dip. This does not, however, rule out contributions from other fac-
268 tors.

269 Figure 3 shows the seasonally-resolved response of ozone in the Northern Hemisphere
270 extratropics in the Chapman+2 photochemical-transport model to stratospheric cool-
271 ing, strengthening BDC, tropospheric expansion, and all three together, compared to the
272 Northern Hemisphere ozone response to an abrupt quadrupling of CO₂ in MRI-ESM2-
273 0. We emphasize that the only seasonally-varying boundary condition of the Chapman+2
274 photochemical-transport model is the strength of the BDC, which varies sinusoidally from
275 zero at the summer solstice to twice the annual mean value at the winter solstice (consistent
276 with reanalyses, e.g., Seviour et al., 2012).

277 The lower dip is stronger in winter and weaker in summer (Fig. 3a,b), and this sea-
278 sonality is easier to explain than that of the upper dip. The Chapman+2 photochemical-
279 transport model suggests that this seasonality comes from seasonality in the effects of
280 tropospheric expansion (Fig. 3i,j), and less so from the effects of stratospheric cooling
281 or strengthening BDC. The seasonality of the ozone reduction in the lower dip depends
282 simply on how much ozone is present to be eroded away: the lower dip is larger in win-
283 ter because there is more ozone in the lowermost stratosphere during that time. The ide-
284 alized model has more ozone in winter because of the seasonally stronger downwelling
285 of the BDC.

286 The seasonality of the upper dip is more subtle to explain. This is because there
287 is not much seasonality in the response to tropical tropospheric expansion itself (Fig. 3k,l).
288 In the simple model, the seasonality of the upper dip comes from seasonality in the re-
289 sponse to stratospheric cooling and the strengthening BDC, both of which exhibit larger
290 increases of ozone in winter that mask the upper dip. Stratospheric cooling leads to a
291 larger increase of mid-stratospheric ozone in winter than in summer (Fig. 3e) because
292 the elevated ozone in the upper stratosphere from stratospheric cooling is downwelled
293 more strongly in winter. Strengthening the Brewer-Dobson circulation leads to a stronger
294 increase of ozone in winter because our prescribed fractional increase in the BDC is largest
295 then. (Our seasonally-varying downwelling varies from zero on July 1 to $2\overline{w}_j^*$ on January
296 1, so strengthening the BDC by increasing \overline{w}_j^* has a peak absolute effect on January 1
297 and no effect on July 1.) An open question is whether seasonality in lateral mixing, such

298 as from the Asian summer monsoon anticyclone could be a leading-order contributor to
299 seasonality in the upper dip, a contribution that could be explored in future work. In
300 summary, the upper dip vanishes in winter because it is masked by annually maximal
301 increases of ozone from stratospheric cooling and the strengthening BDC, which both
302 follow as a direct consequence of the climatological peak of the BDC. A schematic of this
303 mechanistic understanding is shown in Fig. 4.

304 The seasonal cycle of the ozone response to a quadrupling of CO₂ includes large
305 cancellation among opposing terms, so it is not surprising that the sign of the ozone re-
306 sponse to a quadrupling of CO₂ is not robustly simulated in this region (Fig. 1). Although
307 the sign is not robust, this paper demonstrates that key aspects of the pattern of the re-
308 sponse, namely the double dip, can be understood. The sign of the response at each lo-
309 cation and throughout the seasonal cycle could be a sensitive indicator for the effects of
310 model disagreements in stratospheric cooling, the strengthening BDC, and tropospheric
311 expansion.

312 Rising CO₂ is not the only perturbation that will affect the ozone layer in the com-
313 ing decades. Ongoing recovery of the ozone hole due to the Montreal Protocol could po-
314 tentially obscure part of the double dip. Fig. S6 compares ozone in two chemistry-climate
315 models (MRI-ESM2-0 and CNRM-ESM2-1) between 2015-2044 and 2071-2100 in the high-
316 development and high-emissions pathway of ssp585. The annually-averaged change in
317 ozone is plotted as well as the change in only DJF or JJA. Recovery of polar ozone from
318 declining CFCs generally dominates the response, although the upper dip from surface
319 warming is evident in the Northern Hemisphere during JJA for both models.

320 **6 Discussion: Implications for filtering global warming using tropopause-** 321 **following coordinates**

322 Filtering out trends in ozone from global warming is of great interest because the
323 residual time series may help reveal the chemical recovery of the ozone layer due to de-
324 clining ozone-depleting substances (Petropavlovskikh et al., 2019). A growing practice
325 intended to remove the impact of warming is to transform ozone trends into tropopause-
326 following coordinates, based on the understanding that the tropopause rises under global
327 warming (Thompson et al., 2021). The use of tropopause-following coordinates has pro-
328 ceeded with different methods reflecting different assumptions. Some studies assess ozone
329 trends in tropopause-following coordinates through most of the stratosphere (Wargan

330 et al., 2018; Bognar et al., 2022), while others restrict tropopause-following coordinates
331 to an empirically-determined region within roughly 5 km of the tropopause (Pan et al.,
332 2004; Hegglin et al., 2008; Millán et al., 2024). The results in this paper suggest precau-
333 tions towards each approach.

334 Using tropopause-following coordinates throughout the stratosphere assumes that
335 ozone is conserved with respect to the local tropopause under dynamical perturbations
336 in tropopause height. Above 25-30 km, however, the ozone layer is typically in photo-
337 chemical equilibrium (e.g., Perliski et al., 1989; Brasseur & Solomon, 2005) where it is
338 unaffected by dynamical anomalies in ozone due to local tropopause variability (Match
339 & Gerber, 2022).

340 Restricting attention to the dynamically-controlled regime below 25-30 km, we have
341 shown that if both tropopauses rise equally, the resulting change in ozone can be approx-
342 imated by a shift with respect to the local tropopause (Figs. 2, 3, S7). Yet, this only works
343 for a uniform rise in both tropopauses, which is not necessarily expected in response to
344 warming. Non-uniform tropopause changes introduce problems: if only the tropical tropopause
345 rises, tropopause-following coordinates in the extratropics cannot capture the resulting
346 upper dip (Fig S7b); if only the extratropical tropopause rises, tropopause-following co-
347 ordinates predict a spurious upper dip (Fig. S7c). There does not exist a single tropopause-
348 following coordinate that can filter out arbitrary changes in tropopause structure.

349 Restricting tropopause-following coordinates to an empirically-determined window
350 near the tropopause can avoid contamination from the photochemically-controlled re-
351 gion, but introduces other challenges. The empirical window is often chosen by using past
352 data of ozone and tropopause heights to identify where tropopause-following coordinates
353 reduce the variance of ozone compared to absolute height coordinates (Hegglin et al., 2008;
354 Millán et al., 2024). This empirical window thus demarcates where the variability in ozone
355 is dominated by variability in extratropical tropopause height, and has generally been
356 found to extend 2-5 km above the extratropical tropopause. Yet, because the empirical
357 window excludes most of the the upper dip, a major part of the warming response oc-
358 curs outside its frame.

7 Conclusions

The extratropical stratospheric ozone response to rising CO₂ has a robust shape: increases in ozone throughout the stratosphere are punctuated by two dips, i.e., reductions in the size of increase, potentially large enough to yield absolute reductions. The upper dip is at 17 km and is strongest in summer, and the lower dip is at 10 km and is strongest in winter. With the use of CMIP6 chemistry-climate model results and the Chapman+2 photochemical-transport model, the double dip has been explained as follows:

- The lower dip results from expansion of the extratropical troposphere. The lower dip is strongest in winter when extratropical lower stratospheric ozone is largest.
- The upper dip results from expansion of the remote tropical troposphere. The upper dip is strongest in summer, whereas it is masked in winter by the annually maximal increases in ozone from stratospheric cooling and the strengthening BDC.

The sensitivity of extratropical lower stratospheric ozone to both local and remote properties of the tropopause complicates the growing practice of using local tropopause-following coordinates to filter out the effects of changes in tropopause height on ozone.

8 Data Availability Statement

Python software version of the Chapman+2 photochemical-transport model is publicly available at [10.5281/zenodo.13412270](https://doi.org/10.5281/zenodo.13412270), along with the run script used to produce the main experiments analyzed herein. CMIP6 data is freely accessible from <https://esgf-node.llnl.gov/search/cmip6/>.

Acknowledgments

This work was supported by the National Science Foundation under Award No. 2120717 and OAC-2004572, and by Schmidt Sciences, as part of the Virtual Earth System Research Institute (VESRI). For the CMIP6 model output, we acknowledge the World Climate Research Programme, the climate modeling groups, and the Earth System Grid Federation (ESGF), as supported by multiple funding agencies.

References

Abalos, M., Randel, W. J., Kinnison, D. E., Garcia, R. R., Abalos, M., Randel,

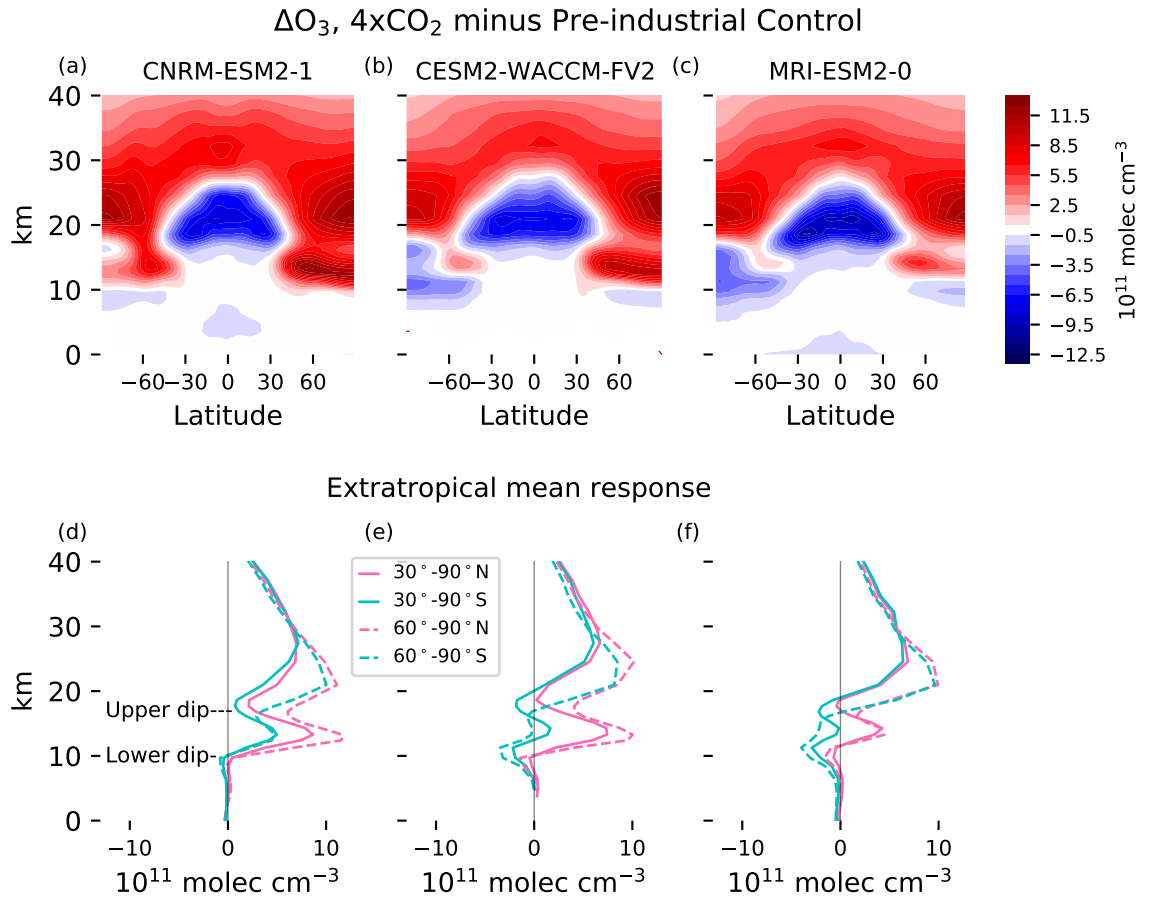


Figure 1. The double dip is evident in the response of extratropical O₃ to a quadrupling of CO₂ in three CMIP6 models with interactive chemistry. Top row: Change in [O₃] in abrupt-4xCO₂ (years 50-150) minus piControl. Bottom row: Extratropical mean changes in [O₃] in the Northern Hemisphere (pink) and Southern Hemisphere (cyan) when averaged poleward of 30° (solid) or poleward of 60° (dashed). The lower dip occurs around 10 km, and the upper dip occurs around 17 km.

387 W. J., ... Garcia, R. R. (2017, October). Using the Artificial Tracer e90 to
 388 Examine Present and Future UTLS Tracer Transport in WACCM. *Journal of*
 389 *the Atmospheric Sciences*, 74(10), 3383–3403. doi: 10.1175/JAS-D-17-0135.1

390 Ball, W. T., Alsing, J., Mortlock, D. J., Staehelin, J., Haigh, J. D., Peter, T., ...
 391 Rozanov, E. V. (2018, February). Evidence for a continuous decline in lower
 392 stratospheric ozone offsetting ozone layer recovery. *Atmospheric Chemistry and*
 393 *Physics*, 18(2), 1379–1394. doi: 10.5194/acp-18-1379-2018

- 394 Ball, W. T., Chiodo, G., Abalos, M., Alsing, J., & Stenke, A. (2020, August). Incon-
395 sistencies between chemistry-climate models and observed lower stratospheric
396 ozone trends since 1998. *Atmospheric Chemistry and Physics*, *20*(16), 9737–
397 9752. doi: 10.5194/ACP-20-9737-2020
- 398 Banerjee, A., C. Maycock, A., T. Archibald, A., Luke Abraham, N., Telford, P.,
399 Braesicke, P., & A. Pyle, J. (2016, March). Drivers of changes in stratospheric
400 and tropospheric ozone between year 2000 and 2100. *Atmospheric Chemistry
401 and Physics*, *16*(5), 2727–2746. doi: 10.5194/ACP-16-2727-2016
- 402 Bognar, K., Tegtmeier, S., Bourassa, A., Roth, C., Warnock, T., Zawada, D., &
403 Degenstein, D. (2022, July). Stratospheric ozone trends for 1984-2021 in the
404 SAGE II-OSIRIS-SAGE III/ISS composite dataset. *Atmospheric Chemistry
405 and Physics*, *22*(14), 9553–9569. doi: 10.5194/ACP-22-9553-2022
- 406 Bönisch, H., Engel, A., Curtius, J., Birner, T., & Hoor, P. (2009, August). Quan-
407 tifying transport into the lowermost stratosphere using simultaneous in-situ
408 measurements of SF₆ and CO₂. *Atmospheric Chemistry and Physics*, *9*(16),
409 5905–5919. doi: 10.5194/acp-9-5905-2009
- 410 Brasseur, G. P., & Solomon, S. (2005). *Aeronomy of the Middle Atmosphere: Chem-
411 istry and Physics of the Stratosphere and Mesosphere*. Dordrecht, Netherlands:
412 Springer.
- 413 Butchart, N. (2014, June). The Brewer-Dobson circulation. *Reviews of Geophysics*,
414 *52*(2), 157–184. doi: 10.1002/2013RG000448
- 415 Chiodo, G., Polvani, L. M., Marsh, D. R., Stenke, A., Ball, W., Rozanov, E., ...
416 Tsigaridis, K. (2018, May). The Response of the Ozone Layer to Quadru-
417 pled CO₂ Concentrations. *Journal of Climate*, *31*(10), 3893–3907. doi:
418 10.1175/JCLI-D-17-0492.1
- 419 Dietmüller, S., Ponater, M., & Sausen, R. (2014, February). Interactive ozone
420 induces a negative feedback in CO₂-driven climate change simulations.
421 *Journal of Geophysical Research: Atmospheres*, *119*(4), 1796–1805. doi:
422 10.1002/2013JD020575
- 423 Fomichev, V. I., Jonsson, A. I., de Grandpré, J., Beagley, S. R., McLandress, C.,
424 Semeniuk, K., & Shepherd, T. G. (2007, April). Response of the Middle At-
425 mosphere to CO₂ Doubling: Results from the Canadian Middle Atmosphere
426 Model. *Journal of Climate*, *20*(7), 1121–1144. doi: 10.1175/JCLI4030.1

- 427 Gettelman, A., Hoor, P., Pan, L. L., Randel, W. J., Hegglin, M. I., & Birner, T.
428 (2011). The Extratropical Upper Troposphere and Lower Stratosphere. *Re-*
429 *views of Geophysics*, 49(3). doi: 10.1029/2011RG000355
- 430 Haigh, J. D., & Pyle, J. A. (1982, July). Ozone perturbation experiments in a two-
431 dimensional circulation model. *Quarterly Journal of the Royal Meteorological*
432 *Society*, 108(457), 551–574. doi: 10.1002/QJ.49710845705
- 433 Hartmann, D. L., & Larson, K. (2002, October). An important constraint on trop-
434 ical cloud - climate feedback. *Geophysical Research Letters*, 29(20), 12-1-12-4.
435 doi: 10.1029/2002gl015835
- 436 Hegglin, M. I., Boone, C. D., Manney, G. L., Shepherd, T. G., Walker, K. A.,
437 Bernath, P. F., . . . Schiller, C. (2008, March). Validation of ACE-FTS satellite
438 data in the upper troposphere/lower stratosphere (UTLS) using non-coincident
439 measurements. *Atmospheric Chemistry and Physics*, 8(6), 1483–1499. doi:
440 10.5194/acp-8-1483-2008
- 441 Holton, J. R., Haynes, P. H., McIntyre, M. E., Douglass, A. R., Rood, R. B., & Pfis-
442 ter, L. (1995). Stratosphere-troposphere exchange. *Reviews of Geophysics*,
443 33(4), 403. doi: 10.1029/95RG02097
- 444 Hoor, P., Gurk, C., Brunner, D., Hegglin, M. I., Wernli, H., & Fischer, H. (2004,
445 August). Seasonality and extent of extratropical TST derived from in-situ
446 CO measurements during SPURT. *Atmospheric Chemistry and Physics*, 4(5),
447 1427–1442. doi: 10.5194/acp-4-1427-2004
- 448 Jeevanjee, N., & Fueglistaler, S. (2020, February). Simple Spectral Models for Atmo-
449 spheric Radiative Cooling. *Journal of the Atmospheric Sciences*, 77(2), 479–
450 497. doi: 10.1175/JAS-D-18-0347.1
- 451 Jonsson, A. I., de Grandpré, J., Fomichev, V. I., McConnell, J. C., & Beagley, S. R.
452 (2004, December). Doubled CO₂ -induced cooling in the middle atmosphere:
453 Photochemical analysis of the ozone radiative feedback. *Journal of Geophysical*
454 *Research*, 109(D24), D24103. doi: 10.1029/2004JD005093
- 455 Keeble, J., Hassler, B., Banerjee, A., Checa-Garcia, R., Chiodo, G., Davis, S., . . .
456 Wu, T. (2021, March). Evaluating stratospheric ozone and water vapour
457 changes in CMIP6 models from 1850 to 2100. *Atmospheric Chemistry and*
458 *Physics*, 21(6), 5015–5061. doi: 10.5194/ACP-21-5015-2021
- 459 Li, F., Stolarski, R. S., & Newman, P. A. (2009). Stratospheric ozone in the post-

- 460 CFC era. *Atmospheric Chemistry and Physics*, 9(6), 2207–2213. doi: 10.5194/
461 ACP-9-2207-2009
- 462 Manabe, S., & Wetherald, R. T. (1967, May). Thermal Equilibrium of the At-
463 mosphere with a Given Distribution of Relative Humidity. *Journal of the At-*
464 *mospheric Sciences*, 24(3), 241–259. doi: 10.1175/1520-0469(1967)024<0241:
465 TEOTAW>2.0.CO;2
- 466 Match, A., & Fueglistaler, S. (2021, December). Large Internal Variabil-
467 ity Dominates over Global Warming Signal in Observed Lower Strato-
468 spheric QBO Amplitude. *Journal of Climate*, 34(24), 9823–9836. doi:
469 10.1175/JCLI-D-21-0270.1
- 470 Match, A., Gerber, E., & Fueglistaler, S. (2024a, January). Beyond self-healing: Sta-
471 bilizing and destabilizing photochemical adjustment of the ozone layer. *EGU-*
472 *sphere*, 1–28. doi: 10.5194/egusphere-2024-147
- 473 Match, A., & Gerber, E. P. (2022, October). Tropospheric Expansion Under Global
474 Warming Reduces Tropical Lower Stratospheric Ozone. *Geophysical Research*
475 *Letters*, 49(19), e2022GL099463. doi: 10.1029/2022GL099463
- 476 Match, A., Gerber, E. P., & Fueglistaler, S. (2024b, June). Protection without poi-
477 son: Why tropical ozone maximizes in the interior of the atmosphere. *EGU-*
478 *sphere*, 1–29. doi: 10.5194/egusphere-2024-1552
- 479 McKim, B. A., Jeevanjee, N., Vallis, G. K., & Lewis, N. T. (2024, February). *Water*
480 *vapor spectroscopy and thermodynamics constrain Earth’s tropopause tempera-*
481 *ture* (Preprint). Preprints. doi: 10.22541/essoar.170904795.55675140/v1
- 482 Millán, L. F., Hoor, P., Hegglin, M. I., Manney, G. L., Boenisch, H., Jeffery, P., . . .
483 Walker, K. (2024, July). Exploring ozone variability in the upper troposphere
484 and lower stratosphere using dynamical coordinates. *Atmospheric Chemistry*
485 *and Physics*, 24(13), 7927–7959. doi: 10.5194/acp-24-7927-2024
- 486 Neu, J. L., & Plumb, R. A. (1999, August). Age of air in a “leaky pipe” model
487 of stratospheric transport. *Journal of Geophysical Research*, 104(D16), 19243.
488 doi: 10.1029/1999JD900251
- 489 Oberländer-Hayn, S., Gerber, E. P., Abalichin, J., Akiyoshi, H., Kerschbaumer, A.,
490 Kubin, A., . . . Oman, L. D. (2016). Is the Brewer-Dobson circulation in-
491 creasing, or moving upward? *Geophysical Research Letters*, n/a-n/a. doi:
492 10.1002/2015GL067545

- 493 Orbe, C., Wargan, K., Pawson, S., & Oman, L. D. (2020). Mechanisms Linked to
494 Recent Ozone Decreases in the Northern Hemisphere Lower Stratosphere.
495 *Journal of Geophysical Research: Atmospheres*, *125*(9), e2019JD031631.
496 (e2019JD031631 10.1029/2019JD031631) doi: 10.1029/2019JD031631
- 497 Pan, L. L., Randel, W. J., Gary, B. L., Mahoney, M. J., & Hints, E. J. (2004).
498 Definitions and sharpness of the extratropical tropopause: A trace gas per-
499 spective. *Journal of Geophysical Research: Atmospheres*, *109*(D23). doi:
500 10.1029/2004JD004982
- 501 Perliski, L. M., Solomon, S., & London, J. (1989, December). On the interpreta-
502 tion of seasonal variations of stratospheric ozone. *Planetary and Space Science*,
503 *37*(12), 1527–1538. doi: 10.1016/0032-0633(89)90143-8
- 504 Petropavlovskikh, I., Godin-Beekmann, S., Hubert, D., Damadeo, R., Hassler, B., &
505 Sofieva, V. (2019). *SPARC/I03C/GAW Report on Long-Term Ozone Trends*
506 *and Uncertainties in the Stratosphere* (Tech. Rep.). SPARC/I03C/GAW.
- 507 Plummer, D. A., Scinocca, J. F., Shepherd, T. G., Reader, M. C., & Jonsson, A. I.
508 (2010). Quantifying the contributions to stratospheric ozone changes from
509 ozone depleting substances and greenhouse gases. *Atmos. Chem. Phys*, *10*,
510 8803–8820. doi: 10.5194/acp-10-8803-2010
- 511 Seeley, J. T., Jeevanjee, N., & Romps, D. M. (2019, February). FAT or FiTT: Are
512 Anvil Clouds or the Tropopause Temperature Invariant? *Geophysical Research*
513 *Letters*, *46*(3), 1842–1850. doi: 10.1029/2018GL080096
- 514 Seviour, W. J. M., Butchart, N., & Hardiman, S. C. (2012, April). The Brewer-
515 Dobson circulation inferred from ERA-Interim. *Quarterly Journal of the Royal*
516 *Meteorological Society*, *138*(665), 878–888. doi: 10.1002/qj.966
- 517 Shepherd, T. G. (2008, January). Dynamics, stratospheric ozone, and climate
518 change. *Atmosphere-Ocean*, *46*(1), 117–138. doi: 10.3137/ao.460106
- 519 Singh, M. S., & O’Gorman, P. A. (2012, December). Upward shift of the atmo-
520 spheric general circulation under global warming: Theory and simulations.
521 *Journal of Climate*, *25*(23), 8259–8276. doi: 10.1175/JCLI-D-11-00699.1
- 522 Stolarski, R. S., Waugh, D. W., Wang, L., Oman, L. D., Douglass, A. R., & New-
523 man, P. A. (2014, May). Seasonal variation of ozone in the tropical
524 lower stratosphere: Southern tropics are different from northern tropics.
525 *Journal of Geophysical Research: Atmospheres*, *119*(10), 6196–6206. doi:

526 10.1002/2013JD021294

527 Thompson, A. M., Stauffer, R. M., Wargan, K., Witte, J. C., Kollonige, D. E., &
528 Ziemke, J. R. (2021, November). Regional and Seasonal Trends in Tropical
529 Ozone From SHADOZ Profiles: Reference for Models and Satellite Products.
530 *Journal of Geophysical Research: Atmospheres*, *126*(22), e2021JD034691. doi:
531 10.1029/2021JD034691

532 Vallis, G. K., Zurita-Gotor, P., Cairns, C., & Kidston, J. (2015, July). Response of
533 the large-scale structure of the atmosphere to global warming. *Quarterly Jour-*
534 *nal of the Royal Meteorological Society*, *141*(690), 1479–1501. doi: 10.1002/qj
535 .2456

536 Wargan, K., Orbe, C., Pawson, S., Ziemke, J. R., Oman, L. D., Olsen, M. A., ...
537 Emma Knowland, K. (2018, May). Recent Decline in Extratropical Lower
538 Stratospheric Ozone Attributed to Circulation Changes. *Geophysical Research*
539 *Letters*, *45*(10), 5166–5176. doi: 10.1029/2018GL077406

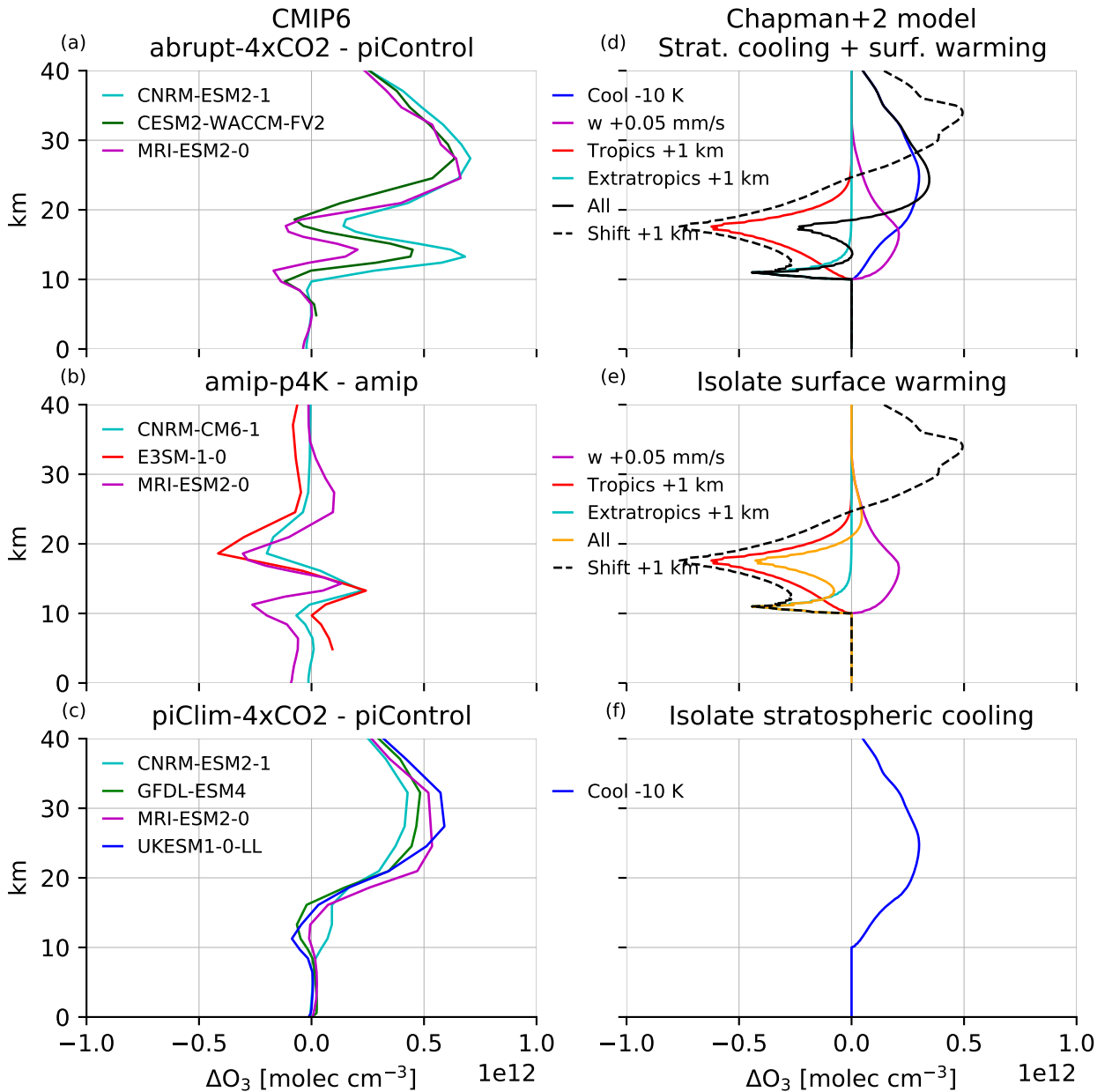


Figure 2. Decomposing the mechanisms by which increasing CO₂ affects extratropical O₃ in CMIP6 models (left column) and the Chapman+2 model (an idealized photochemical-transport model, right column). (a) Response of extratropical O₃, averaged poleward of 30°, to abrupt-4xCO₂ minus piControl in the three CMIP6 models shown in Fig. 1. (b) As above, but isolating surface warming through amip-p4K minus amip. (c) As above, but isolating stratospheric cooling through piClim-4xCO₂ minus piControl. The double dip is due to surface warming and not stratospheric cooling. (Right column) Extratropical O₃ response to the key mechanistic drivers of the response: stratospheric cooling of 10 K (blue), strengthening Brewer-Dobson circulation by 0.05 mm s⁻¹ (magenta), expansion of the tropical troposphere by 1 km (red), expansion of the extratropical troposphere by 1 km (cyan), and all together (black). (Dashed black) Change in O₃ from a 1 km upward shift of the control profile. The lower dip is due to expansion of the extratropical troposphere, and the upper dip is due to expansion of the tropical troposphere.

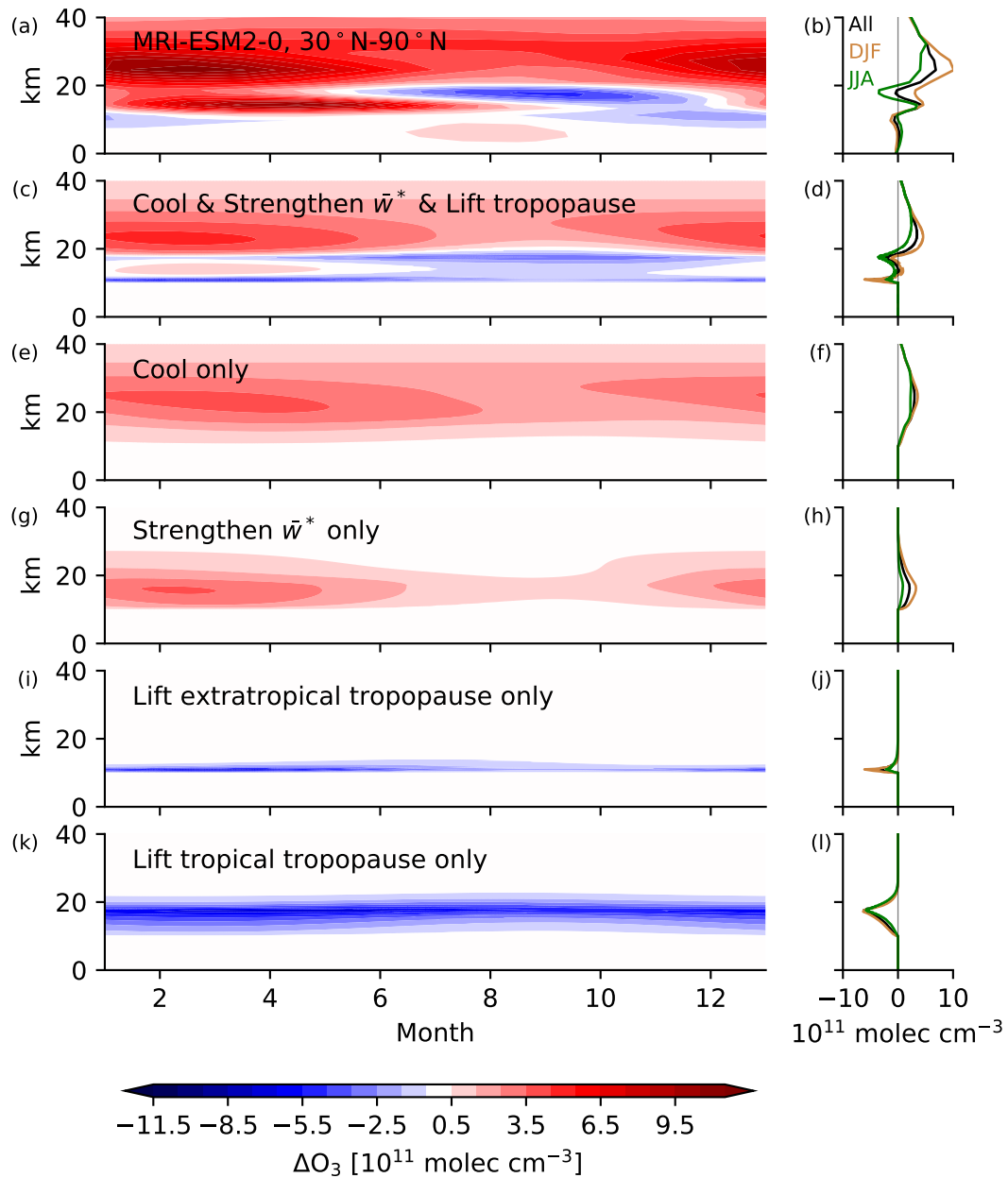


Figure 3. Mechanistic decomposition of the annual cycle in the Northern Hemisphere extratropical O_3 response to global warming. (Left column) (a) MRI-ESM2-0 for abrupt-4xCO2 minus piControl and (c,e,g,i,k) Chapman+2 mechanism denial experiments, in which all seasonality arises solely from a prescribed annual cycle in the Brewer-Dobson Circulation (strongest in winter of each hemisphere). In MRI-ESM2-0, the upper dip around 17 km is strongest in summer whereas the lower dip around 10 km is strongest in winter, with both aspects reproducible from the Chapman+2 model whose sole seasonally-varying driver is BDC strength. (Right column) Temporal average of the left column across All months (black), DJF (brown), and JJA (green).

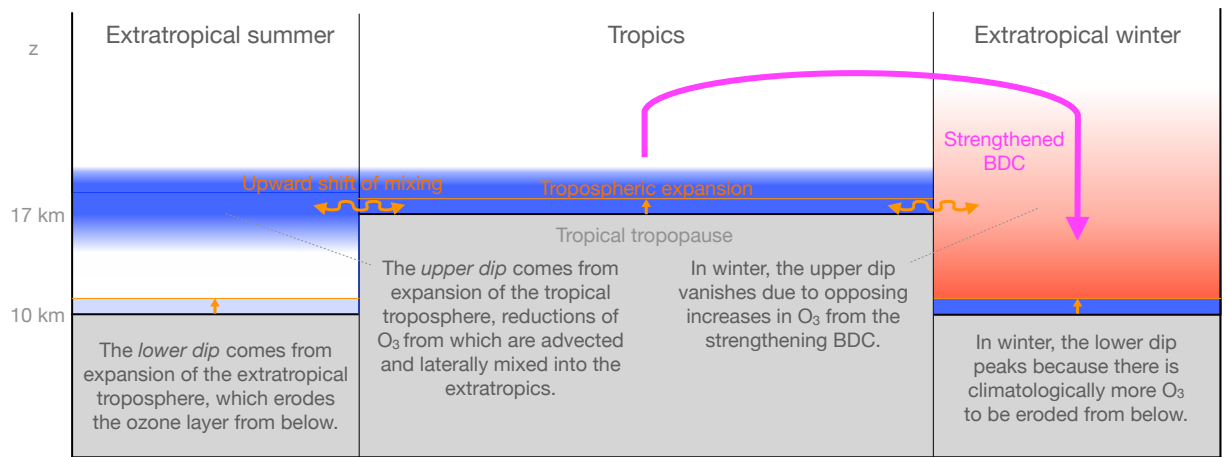


Figure 4. Schematic illustrating how surface warming leads to each dip and its seasonality. Reductions of ozone are in blue and increases are in red.